Experiments for combined solar and heat pump systems

Peter Pärisch[*], Jonas Warmuth, Erik Bertram, Rainer Tepe

Institut für Solarenergieforschung Hameln GmbH, Am Ohrberg 1, 31860 Emmerthal, Germany

[*] Corresponding Author: p.paerisch@isfh.de

Abstract

The operation of ground coupled heat pumps in combination with solar collectors requires comprising knowledge of the component behaviour under non-nominal conditions. Especially higher source and lower sink temperatures, varying flow rates, material characteristics and sophisticated control strategies have to be taken into account.

Therefore stationary and dynamic tests of a heat pump and a borehole heat exchanger system have been carried out in order to analyse the behaviour under varying conditions.

In details the heat pump efficiency depending on temperature and flow rate has been investigated. High source temperatures especially with low sink temperatures lead to a strong decrease in the exergetic efficiency which reduces the expected improvement of the COP significantly. And this effect depends strongly on the temperature difference between sink and source (temperature lift). The lower the temperature lift the stronger the drop in the exergetic efficiency. Varying flow rate only has an influence on temperature boundary conditions not on heat transfer coefficient.

For simulations of systems with solar ground regeneration the polynomial coefficients of the YUM-model (TRNSYS type 401 [1]) must be determined by a sufficient data basis, which includes data on the source side up to 30 °C. The model algorithm based on these coefficients works accurately for the mass flow rate of the data basis but it is not applicable for other flow rates. For this purpose, e. g. the correction method from [9] can be used and gives reasonable results. Based on this method the relative error in COP decreases from 5 % to about 2 %.

Furthermore, temperature step response tests of borehole heat exchangers with different flow rates have been carried out. These tests show that the heat extraction rate at the beginning of the test is a couple of times higher than the steady state value. Both values, the peak and the steady-state value, are increased with higher flow rates but the sensitivity of the peak value is much higher.

1. Introduction

The combination of solar thermal collectors with ground-coupled heat pump systems offers the possibility to reduce the annual electricity demand (e. g. [5], [12]) and to avoid uncertainties in the planning process [3]. However, the solar collector can be connected to the system in several ways: directly to the space heating system or the DHW preparation, to the heat source or to the evaporator of the heat pump. For each option different restrictions for the flow rates, operation temperatures and control strategies have to be taken into account.

In order to analyse these effects several tests have been carried out at the variable test facility for heat pumps and borehole heat exchangers at the ISFH (see [10] for further information). This test rig has

been built up within the joint project Geo-Solar-WP focusing on "High-efficient heat pump systems with geothermal and solar thermal energy sources" that is funded by the European Union and the Federal State of Lower Saxony.

In addition, the experiments will be supported by TRNSYS simulations. First of all, these simulations shall replicate the test itself. Secondly, they are used to analyse the performance of different simulation models and, third, thus allow studying the behaviour of different system combinations, like in [4].

2. Heat pumps in combined solar and geothermal systems

Solar heat injection can either be realised on the source or the sink side of the heat pump. In both cases the operating temperatures of the heat pump will be influenced. By delivering heat to the source side the evaporator temperature will be increased, which has a positive effect on the heat pump efficiency. On the other hand heat delivered directly to the sink side avoids heat pump running time and can affect the average condenser temperature in both directions. For example, a solar DHW-system avoids heat pump running time for DHW preparation and thus will reduce the mean condenser temperature if the heating system operates on lower temperature levels.

2.1 Sensitivity of heat pump efficiency concerning flow and temperature variations

A brine/water heat pump with thermostatic expansion valve has been measured in the test system with different flow rates and inlet and outlet temperatures. The hydraulic scheme including the measured values is shown in Fig. 1. The heat pump is connected to computer controlled hydraulic modules that regulate constant temperatures, constant heat flow rates and constant mass flow rates as well.
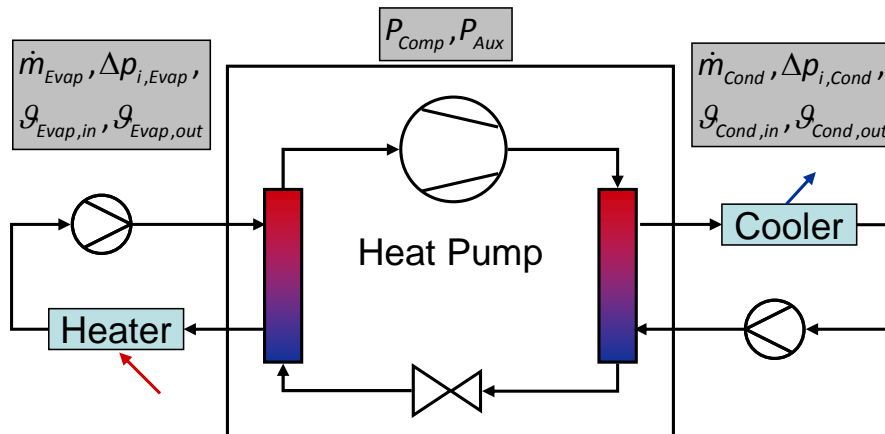

Fig. 1 Hydraulic scheme of the test system and measured values

Unlike the requirements in the European Standard DIN EN 14511-3 [6] the steady-state is measured with nominal flow rates and kept stable only for 25 to 30 minutes. The standard deviations of the single temperature values of the sliding average during the steady-state are below 0.2 K. The realised uncertainties of the measurements can be seen in Table 1 in comparison to the standards values.

Table 1: Required and realised uncertainties of measurement [6]

Measured value	ISFH	DIN EN 14511-3
Heat flux	- (here 0.44-1.47 %)	5 %
Compressor power	0.04 kW (here 1.87-3.66 %)	1 %
COP	- (here 1.96-3.96 %)	-
Temperatures	0.064 K	0.15 K
Mass flow rate source	0.1 %	1 %
Mass flow rate sink	0.2 %	1 %
Concentration Brine	1.6 %	2 %
Pressure drop evaporator	(here ≈37,1 %)	5 %
Pressure drop condenser	(here ≈16,5 %)	5 %

First published results according to EN 14511-3 [7] with constant inlet temperatures of the evaporator and **constant outlet temperatures** of the condenser have showed that the efficiency of the heat pump is only slightly depending on the evaporator mass flow rate [10].

Further investigations have revealed that the change in the temperature difference of the condenser due to flow rate variations can't be neglected. Thus, for the analysis of the heat pump characteristics depending on condenser mass flow rate other tests with constant **average condenser temperatures** $\overline{\vartheta_{Cond}}$ have been carried out (see [11]).

Here, the tests have been conducted for three different **condenser inlet temperatures** (45 °C, 35 °C and 25 °C) and eight different evaporator inlet temperatures (-5 °C to 30 °C in 5 K-steps).
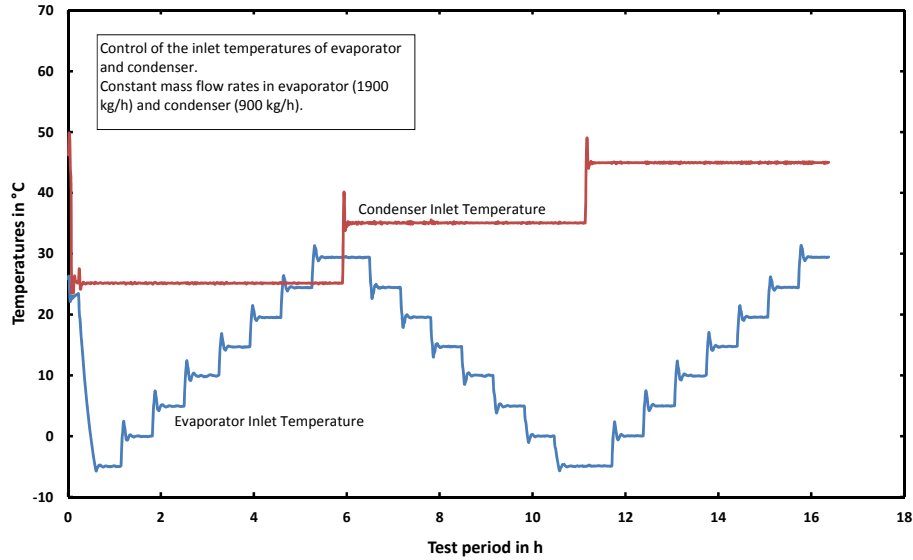
Fig. 2: Temperatures during a test sequence for the determination of the heat pump characteristics

The coefficient of performance COP for heat pumps for space heating without integrated circulation pumps follows from Eq. 1 according to DIN EN 14511-3 [6]. The standard aims at making the heat pumps comparable. Therefore internal circulation pumps are added, if not yet integrated, that only overcome the internal pressure drop Δp_i. The indices „Cond", „Evap", „Comp" and „Aux" stand for condenser, evaporator, compressor and controller.

$$COP = \frac{\dot{Q}_{Cond} + \dfrac{\Delta p_{i,Cond} \cdot V_{Cond}}{\eta_{P,Cond}}}{P_{Comp} + P_{Aux} + \dfrac{\Delta p_{i,Evao} \cdot V_{Evao}}{\eta_{P,Evap}} + \dfrac{\Delta p_{i,Cond} \cdot V_{Cond}}{\eta_{P,Cond}}}$$

Eq. 1

η_P is the efficiency of the circulation pumps for sink and source side that is calculated according to the latest version of DIN EN 14511-3 [6] depending on the hydraulic power of the circulation pumps P_{hydr} (in W):

$$\eta_P = 0{,}0721 \cdot P_{hydr}^{0,3183}$$

Eq. 2

Measured COP values according to Eq. 1 with its standard uncertainties are shown in Fig. 3 for different test conditions. The standard uncertainties of the COP lie between 2 and 4 %. It is obvious that the heat pump efficiency is better for higher source temperatures and lower sink temperatures which are both influenced by solar heat injection (no. 1 and 2 in Fig. 3).

1. Solar heat injection to the source side leads to higher evaporator temperatures and thereby has a positive effect on the efficiency of the heat pump. Furthermore, the heat source benefits indirectly from solar heat supply to the sink side due to less heat extraction from the ground.

2. However solar heat injection to the condenser side can affect the mean condenser temperature in both directions. A solar preheating of the return temperature of the heating system leads to higher inlet temperatures into the condenser and thereby to decreased COP-values. On the other hand the mean condenser inlet temperature will decrease if e. g. a significant part of the DHW-demand is covered by a solar collector and furthermore the temperature of the heat distribution system is below the mean temperature level for DHW preparation. Thus the operation conditions for the heat pump are improved and better COP-values will be reached.

It has to be stated that these considerations mainly focus on the COP or the seasonal performance factor of the heat pump (SPF_{HP}) itself. The effect on the SPF of the complete heating system (SPF_{SHP}) may be different.
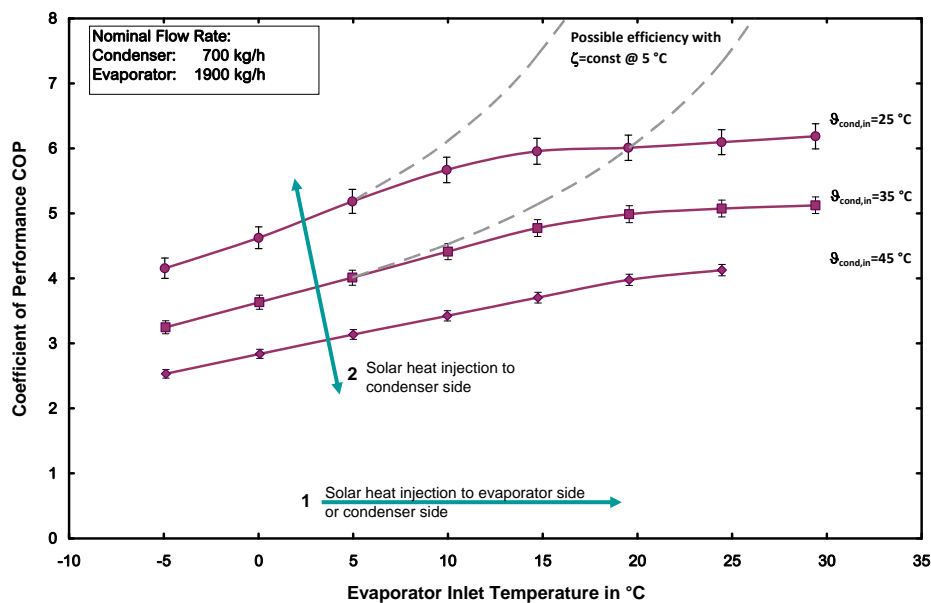

Fig. 3: Coefficient of performance at nominal mass flow rates for three different mean condenser temperatures over the evaporator inlet temperature and theoretic COP if exergetic efficiency ζ is assumed to be constant (e. g. @ 5 °C)

Furthermore Fig. 3 shows the expected COP if the quality grade or exergetic efficiency ζ (see [2]) is assumed to be constant (here based on the values of 5 °C source temperature). The deviation between real and theoretic COP becomes huge for higher source temperatures which is obvious due to the design of the heat pump for typical operation conditions. However, the effect is contrary to the basic idea to improve the system performance by higher source temperatures.

2.2 Flow dependency of heat pump efficiency
Characteristic curves for different mass flow rates on source or sink side are shown in Fig. 4. The flow rate variation of the evaporator is presented in the right diagram and of the condenser side in the left diagram. The shift of the curves for the mass flow rate variation is caused by two effects, both influencing the heat transfer coefficient and the temperature levels of the inlet and outlet flows.
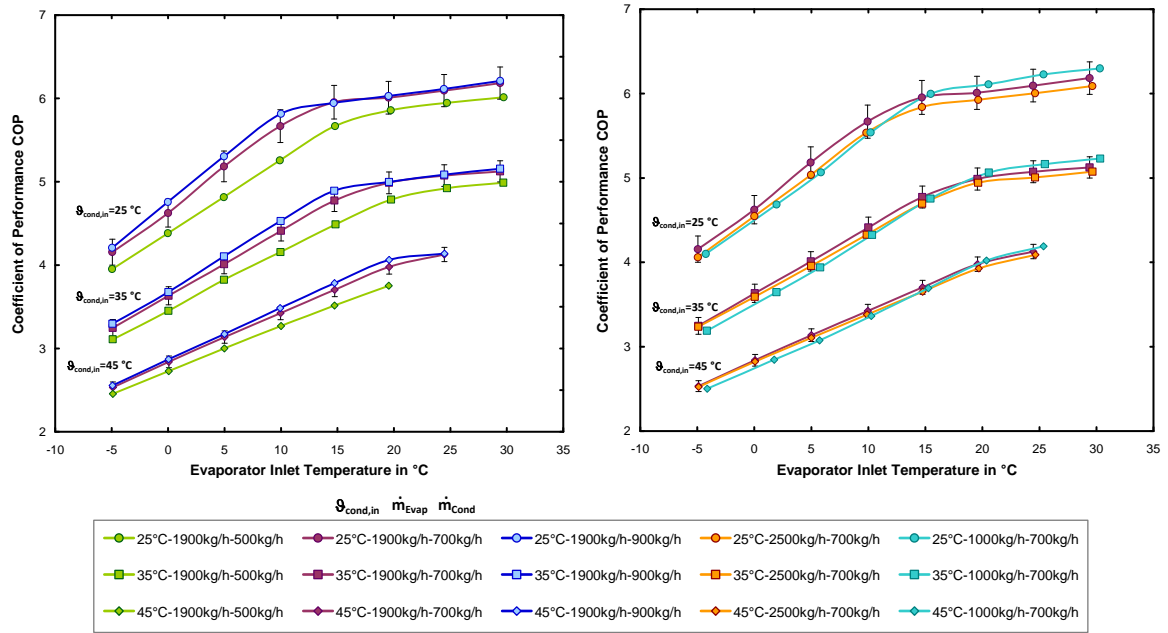
Fig. 4: Coefficient of performance at nominal mass flow rate in the evaporator over varying evaporator inlet temperatures for three different condenser flow rates and mean condenser temperatures

In order to divide between the two effects the exergetic efficiency ζ is calculated by dividing the COP by the maximum possible COP.

$$\zeta = \frac{COP}{COP_{max}}$$

Eq. 3

The maximum possible COP for Carnot cyclic processes follows from:

$$COP_{max} = \frac{T_{Cond,m}}{T_{Cond,m} - T_{Evap,m}}$$

Eq. 4

Here the thermodynamic mean temperature T_m after [2] for evaporator and condenser is used. Eq. 5 shows for example the thermodynamic mean temperature of the condenser.

$$T_{Cond,m} = \frac{T_{Cond,out} - T_{Cond,in}}{\ln\left(\frac{T_{Cond,out}}{T_{Cond,in}}\right)}$$

Eq. 5

The exergetic efficiency allows eliminating the effect of the temperature difference. Thus the curves in Fig. 5 show that the effect of different flow rates on the exergetic efficiency is small. And this is independent whether the hydraulic power of the pressure drop Δp_i is considered or not. Hence, the heat pump efficiency is mainly depending on the temperature levels for the inlet and outlet flows, which are determined by the different flow rates.
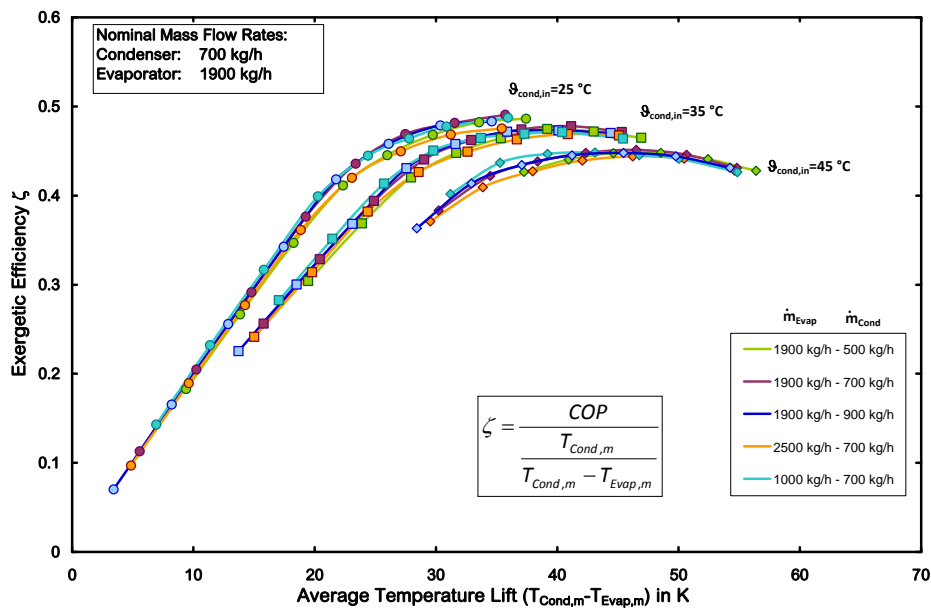
Fig. 5: Exergetic efficiency for different mean condenser temperatures and flow rates over the average temperature lift of the heat pump

The exergetic efficiency in Fig. 5 is plotted over the average temperature lift of the heat pump. The measured data point on the right side of each curve belongs to a source temperature of -5 °C and the source temperature is rising from the right to the left. The optima of the exergetic efficiency curves lie at a temperature lift of about 35 to 45 K between sink and source. A reduction of the temperature lift below the optimum by solar heat supply on the source side leads to a decrease in exergetic efficiency and the COP-values approximately reach constant values (see Fig. 3 and Fig. 4). The exergetic optimum is shifted to higher values with higher condenser temperatures.

To conclude, solar heat supplied to the source side of heat pump systems with high condenser temperatures is more valuable and leads to higher electricity savings than in systems with low condenser temperatures.

In order to quantify the COP improvement depending on the source temperature rise the COP characteristic curves are differentiated (see Fig. 6) with respect to the temperature difference. This relative COP-gain is related to electrical energy savings.

All the curves in Fig. 3 to Fig. 5 and especially in Fig. 6 express an effect that can't be neglected if a solar collector shall be connected to a ground coupled heat pump system: solar heat that is used to increase the evaporator inlet temperature does not always lead to significant improvements in the system performance (between 0.3 and 2.5 %/K). Especially for low temperature lifts between evaporator and condenser the possible gains from solar heat supply is abolished by characteristic heat pump behaviour. In addition, systems that combine both technologies should be equipped with controllers that use sophisticated algorithms which include the knowledge about heat pump characteristics in a broad temperature band (see [8] for an example).
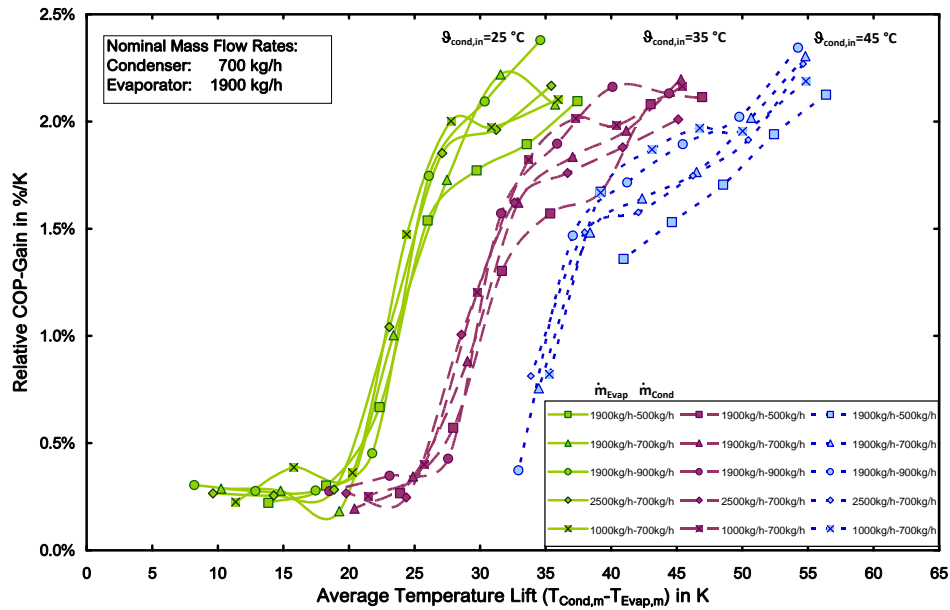
Fig. 6: Relative COP-gain per K increase of the source temperature as a function of average temperature lift for different configurations of flow rate and condenser inlet temperatures

3 Validation of YUM-heat pump model (TRNSYS Type 401)

The TRNSYS Type 401 [1] is a black-box model for compression heat pumps that works with biquadratic polynomials describing the temperature dependency of the condenser power and the electric power. The 12 required coefficients (6 for condenser and 6 for electric power) are calculated by a multi-linear regression of manufacturer or test centre data. Of course the variation of the data, at least 12 points, should cover the whole temperature range of the expected heat pump operation to avoid extrapolation. As well, to cover a broader temperature range as it might occur in combined systems with solar thermal collectors the amount of interpolation nodes of the polynomials should be high. Here 23 interpolation nodes at nominal flow rates are used.

For the validation of Type 401 the measured mass flow rates and the inlet temperatures of evaporator and condenser of the experiments above (see Fig. 2) are given as input values into the model. Then the deviations between simulated and measured thermal and electric power and COP are compared (see Polynomial 700 Test 700 data in Fig. 7).

In general, Type 401 is made for heat pump operation with constant flow rates. However, in combined systems it might be necessary to run the components with varying flow rates. The investigations have shown that Type 401 works most precisely for constant flow rates and with polynomial coefficients determined on basis of the same operation conditions. For a system operation with varying flow rates [9] show a method how the polynomial coefficients only from the reference case can be applied indeed.

The first boundary condition to derive the correction formulas is constant mean temperature:

$$\frac{\vartheta_{out} + \vartheta_{in}}{2} = \frac{\vartheta'_{out} + \vartheta'_{in}}{2}$$

Eq. 6

The second boundary condition is constant heat flow rate. Assuming that the influence of the fluid heat capacity can be neglected due to Eq. 6 it follows simplified (here for the evaporator):

$$\dot{m}_{in} \cdot \left(\vartheta_{in} - \vartheta_{out}\right) = \dot{m}'_{ref} \cdot \left(\vartheta'_{in} - \vartheta'_{out}\right)$$

Eq. 7

Based on these conditions, the method leads finally to the two following formulas, Eq. 8 for the corrected inlet temperature and Eq. 9 for the "re-corrected" outlet temperature:

$$\vartheta'_{in} = \vartheta'_{out} \cdot \frac{\dot{m}'_{ref} - \dot{m}_{in}}{\dot{m}'_{ref} + \dot{m}_{in}} + \vartheta_{in} \cdot 2 \cdot \frac{\dot{m}_{in}}{\dot{m}'_{ref} + \dot{m}_{in}}$$

Eq. 8

$$\vartheta_{out} = \vartheta_{in} \cdot \frac{\dot{m}_{in} - \dot{m}'_{ref}}{\dot{m}'_{ref} + \dot{m}_{in}} + \vartheta'_{out} \cdot 2 \cdot \frac{\dot{m}'_{ref}}{\dot{m}'_{ref} + \dot{m}_{in}}$$

Eq. 9

The validation of the YUM-Model including the flow rate correction according to [9] is carried out in several steps:

1. The polynomial coefficients are determined from the steady-state data at constant flow rate conditions (condenser 500, 700 or 900 kg/h each with evaporator 1900 kg/h). Afterward the model with the polynomial coefficients is applied to the whole measured data set (including instationary values see Fig. 2) with the **correct** flow rate in order to determine the uncertainty of the model (Abbreviations in Fig. 7 „Polynomial700 Test700", „Polynomial500 Test500" „Polynomial900 Test900"). These deviations represent the optimum and therefore the reference for a flow rate correction. The average relative deviation of the model for the three different condenser flow rates is shown in Table 2.

Table 2: Model uncertainty for condenser heat flow rate, electric power and COP, average for three flow rates (condenser 500, 700, 900 kg/h, evaporator 1900 kg/h) between measurement and simulation

		$\dot{Q}_{Cond}$	P_{el}	COP
Relative deviation	%	0.64%	-0.26%	1.14%
Standard deviation	%	3.6%	3.6%	5.4%

2. In the second step the model is fed with the coefficients derived with nominal flow rate but applied to the measured data set of another flow rate (abbreviations in Fig. 7 „Polynomial700 Test500" „Polynomial700 Test900") in order to determine the error due to **"wrong" coefficients**. The errors of the condenser heat flow rate and the electric power increase from 1 up to 3 %. The error of the COP increases even up to 5 %.
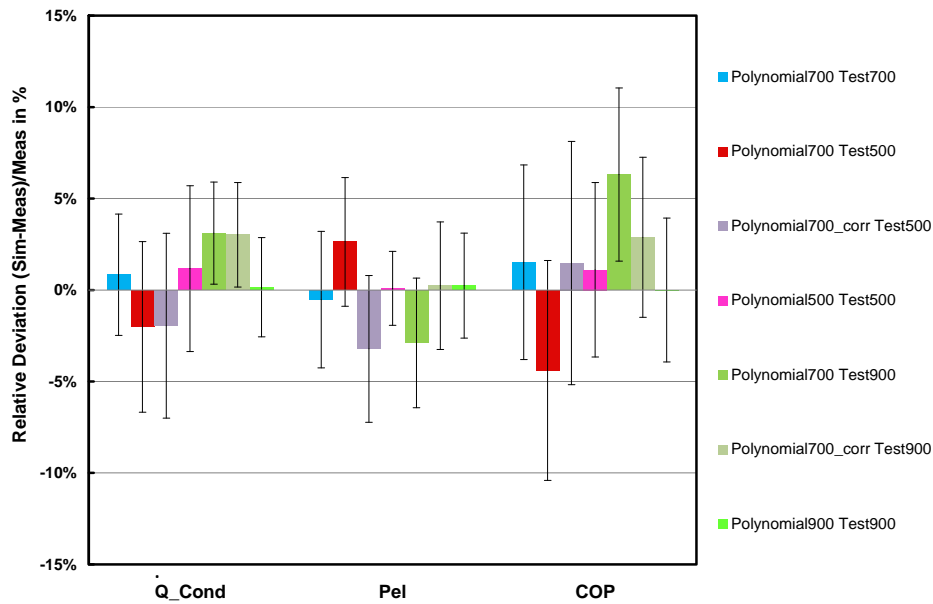
Fig. 7: Relative deviation and standard deviation between simulation and measurement for condenser heat flow rate, electric power and COP for different pairs of polynomial coefficients and flow rates

3. Finally the **flow rate correction** according to [9] is analysed. Obviously the model error due to „wrong" coefficients obtained from 700 kg/h data applied to 500 kg/h and 900 kg/h data (abbreviation in Fig. 7 „Polynomial700_corr Test500" „Polynomial700_corr Test900") decreases. The error of the COP is reduced from 5 % to about 2 %. The improvement considering $\dot{Q}_{cond}$ and P_{el} is less big. It can be stated that the correction methods is applicable and leads to better results.

4. Dynamic behaviour of borehole heat exchangers

Furthermore the dynamic behaviour of borehole heat exchangers (BHE) is investigated by temperature step responses with variable mass flow rates. The test is carried out in two phases.

First, the heat pump cools down the source storage (300 l) to a temperature of about -8 °C in order to have a peak load buffer. Second, the BHE operation starts and the fluid flows through the source storage and via an electric heater back to the ground. The electric heater is needed to hold the desired BHE inlet temperature of -2 °C. The temperature in the ground around the BHE is nearly the undisturbed ground temperature (≈10.8 °C) in the beginning of every experiment. Every test is operated with different flow rates and stopped after 15 kWh have been extracted. Fig. 8 shows the measured specific heat extraction rates.
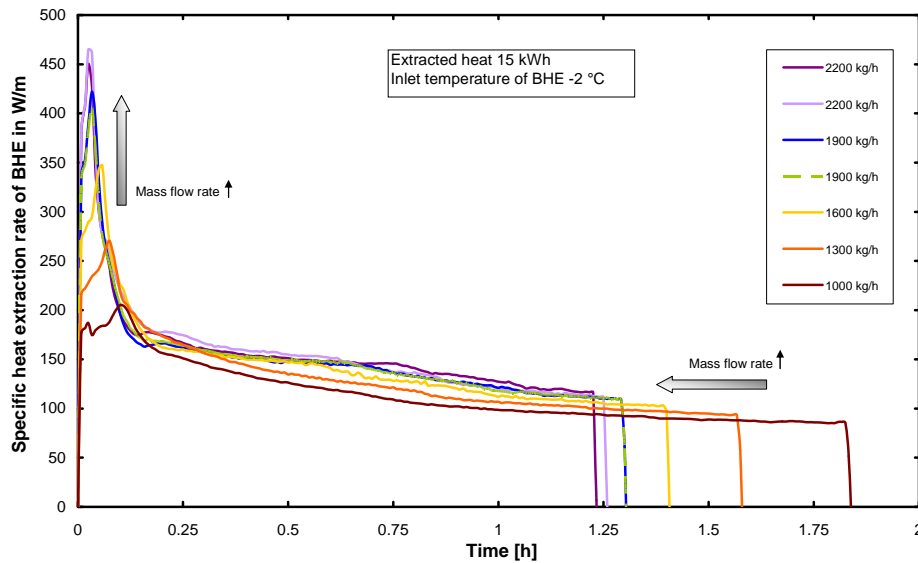
Fig. 8: Specific heat extraction rates of BHE during a temperature step response with variable flow rate

It is obvious that the heat extraction rate increases to very high values at the beginning of the test due to capacity effects during discharging of the BHE. Behind the peak the heat extraction rate decreases hyperbolically to a steady value which is not reached during the test.
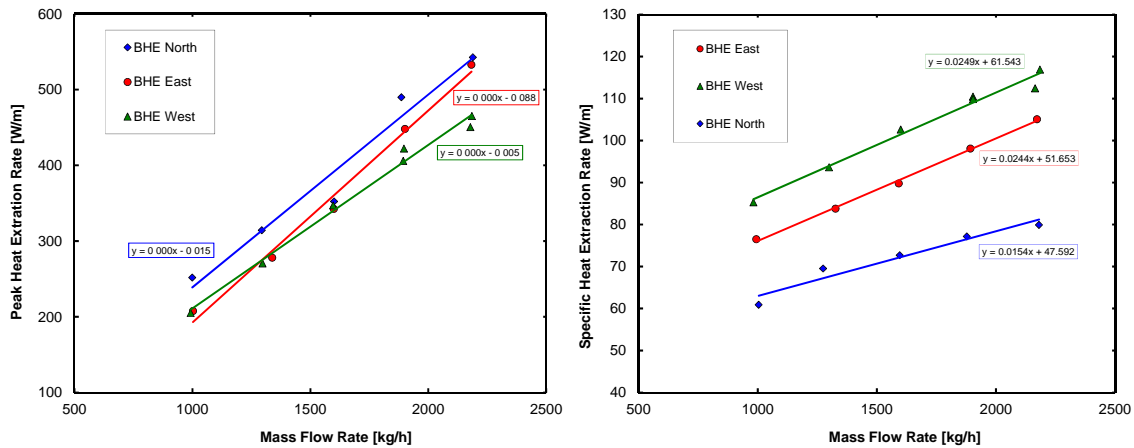

Fig. 9: Specific peak value of heat extraction (left) and heat extraction rate at the end (right) of a temperature step response with -2 °C inlet temperature and extracted heat of 15 kWh

The specific peak value (in Fig. 9 on the left) and the specific heat extraction rates at the end of the test (in Fig. 9 on the right) increase with higher mass flow rates leading, of course, to an earlier finish of the test (see Fig. 8). The peak value is more sensitive to flow rate variation than the heat extraction rate at the end of the test. By doubling the mass flow rate the peak value is doubled as well, while the extraction rate at the end of the test increases only by 30 %.

These capacity effects may be used in sophisticated operation strategies like start-stop strategies with one or more borehole heat exchangers, with modulating heat pumps and with source storage. Further investigations will be carried out using dynamic system simulation tools in order to analyse the potential of such intermediate control strategies.

Acknowledgement

References

[1]   Afjei, T. and Wetter, M. 1997. *Compressor heat pump including frost and cycle losses. Version 1.1 Model description and implementing into TRNSYS*. Zentralschweizerisches Technikum Luzern.

[2]   Baehr, H.D. and Kabelac, S. 2009. *Thermodynamik*. Springer.

[3]   Bertram, E., Glembin, J., Scheuren, J., Rockendorf, G. and Zienterra, G. 2008. Unglazed Solar Collectors in Heat Pump Systems: Measurement, Simulation and Dimensioning. (Lisbon, Portugal, Oct. 2008).

[4]   Bertram, E., Pärisch, P. and Tepe, R. 2012. Impact of solar heat pump system concepts on seasonal performance - Simulation studies. *Proceedings of the EuroSun 2012 Conference* (Rijeka, Croatia, 20.09. 2012).

[5]   Bertram, E., Stegmann, M. and Rockendorf, G. 2011. Heat Pump Systems with Borehole Heat Exchanger and Unglazed PVT Collector. *Proceedings of the ISES Solar World Congress 2011* (Kassel, Germany, 08.-02.09. 2011).

[6]   DIN EN 14511-3 2012. Luftkonditionierer, Flüssigkeitskühlsätze und Wärmepumpen mit elektrisch angetriebenen Verdichtern für die Raumbeheizung und Kühlung - Teil 3: Prüfverfahren. Beuth.

[7]   DIN EN 14511-3 2008. Luftkonditionierer, Flüssigkeitskühlsätze und Wärmepumpen mit elektrisch angetriebenen Verdichtern für die Raumbeheizung und Kühlung - Teil 3: Prüfverfahren. Beuth.

[8]   Haller, M. and Frank, E. 2011. On the potential of using heat from solar thermal collectors for heat pump evaporators. *Proceedings of the ISES Solar World Congress 2011* (Kassel, Germany, 08.-02.09. 2011).

[9]   Pahud, D. and Lachal, B. 2004. *Mesure des performances thermiques d'une pompe à chaleur couplée sur les sondes géothermiques à Lugano (TI)*. Technical Report #40430 / 80266. Bundesamt für Energie.

[10] Pärisch, P., Kirchner, M., Wetzel, W., Voß, S. and Tepe, R. 2011. Test system for the investigation of the synergy potential of solar collectors and borehole heat exchangers in heat pump systems. *Proceedings of the ISES Solar World Congress 2011* (Kassel, 08.-02.09. 2011).

[11] Pärisch, P., Warmuth, J., Kirchner, M. and Tepe, R. 2012. Durchfluss- und Temperaturabhängigkeit von Wärmepumpen im Projekt "Hocheffiziente Wärmepumpensysteme mit Geothermie- und Solarthermie-Nutzung." *Tagungsband des 22. Symposiums Thermische Solarenergie* (Bad Staffelstein, 4.5. 2012).

[12] Tepe, R., Rönnelid, M. and Perers, B. 2003. Swedish Solar Systems in Combination with Heat Pumps. *Proceedings of the ISES Solar World Congress 2003* (Göteborg, 2003).